Prepublished copy

Nature Environment & Pollution Technology

This is a peer-reviewed prepublished version of the paper to be published in Vol. 25, No. 1, March 2026 issue

Original Research

Sunlight-Induced Photocatalytic Degradation of Methyl Red Using Lignocellulosic Biomass of *Ricinus communis* Stem with Isotherm and Kinetic Modeling

V. Nirmala Devi[1]†, B. Jeyagowri[1], S. J. Pradeeba[1], L. Vidhya[1] and N. Nithiya[2]

[1]Department of Chemistry, Hindusthan College of Engineering and Technology, Coimbatore-641032, India

[2]Department of Physics, Hindusthan College of Engineering and Technology, Coimbatore-641032, India

†Corresponding author: V. Nirmala Devi; keerthi16nir@gmail.com

ORCID IDs of Authors:

Dr. V. Nirmala Devi: ORCHID: https://orcid.org/0000-0001-8463-6185

Dr. B. Jeyagowri: ORCHID: https://orcid.org/0000-0002-4252-2785

Dr. S. J. Pradeeba: ORCHID: https://orcid.org/0000-0002-3737-8440

Dr. L. Vidhya: ORCHID: https://orcid.org/0000-0001-6161-1786

Dr. N. Nithiya: ORCHID: https://orcid.org/0000-0003-3545-1955

Key Words	Photocatalysis, *Ricinus communis stem*, Methyl red, Adsorption isotherm, Kinetic studies
DOI	https://doi.org/10.46488/NEPT.2026.v25i01.B4343 (DOI will be active only after the final publication of the paper)
Citation for the Paper	Nirmala Devi, V., Jeyagowri, B., Pradeeba, S. J., Vidhya, L. and Nithiya, N., 2026. Sunlight-induced photocatalytic degradation of methyl red using lignocellulosic biomass of *Ricinus communis* stem with isotherm and kinetic modeling. *Nature Environment and Pollution Technology*, 25(1), p. B4343. https://doi.org/10.46488/NEPT.2026.v25i01.B4343

ABSTRACT

Nowadays, Water pollution is a major global issue brought on by the mixing of effluents from various industries, such as leather, paper, printing cosmetics, Textile etc. containing metal ions and dyes. This impact causes severe damage to the health of human, aquatic plants and animals. In the view of removing the dyes from the wastewater the several techniques available poses certain drawbacks. To combat such issues a rapid, cost effective, eco-friendly and sludge less method for removing dye from the effluent using activated *Ricinus communis* stem as a catalyst in solar irradiation method is discussed and reported with results. The adsorption studies carried out followed by degradation of methyl red onto Si –RCS shows 86% in the presence of natural sunlight

and the optimum dye concentration was 20 ppm at 0.25 g photocatalyst dosage it depicts that the prepared adsorbent material Si-RCS can be used as an effective adsorbent as well as photo catalyst to treat textile effluents. The best fit model was found to be pseudo second order based on the R^2 value. Among the isotherm models studied, it was found that Langmuir is the best fit model.

INTRODUCTION

Water is essential to all life for survival. Water pollution is the tainting of bodies of water, including rivers, lakes, ponds, and groundwater as a result of dumping of sewage, industrial waste, acid rain, oil pollution, thermal power plants, and eutrophication. One of the most significant industrial sector involved in environmental degradation is the textile sector. There are 72 hazardous compounds released into water supplies by the dyeing industry, of which 30 hazardous compounds are difficult to be removed. Each year, more than 10,000 dyes are used in the textile, leather, paper, rubber, cosmetic, pharmaceutical, plastic, and food industries (Monda, 2018). The dye-containing wastewater breaks down into cancer-causing aromatic amines in the absence of dissolved oxygen which adversely affects the animals, plants, and humans (Rimsha Jameel et al. 2024). Sludge, industrial waste, and radioactive waste disposal contributes pollutes around 70% of the water resources. Since dyes are typically mutagenic, carcinogenic, and poisonous by nature, industrial effluents should be treated before being released into the environment (Hameed and El-Khaiary, 2008).

When these textile effluents are ingested by aquatic species through the food chain, it can cause a number of physiological abnormalities, including kidney damage, hypertension, cramps, and occasional fever (Karthikeyan et al. 2006). A risk to survival arises from the buildup of dyes in biotic and abiotic components. Water pollution is a contributing factor to a number of health issues, including blood disorders, heart conditions, nervous system disorders, skin lesions, vomiting, and diarrhea including chromosomal changes (Galenda et al.. 2014).

Methyl red is a mono azo dye (2-(4-[dimethyl amino] phenyl azo) benzoic acid) used in textile dyeing, paper printing and as indicator in acid base titrations. The discharge of Methyl red from various industries cause harmful effects to human beings, plants, animals and the environment (Vinoda et al. 2015). The direct inhalation of methyl red damages the central nervous system, digestive path irritation, kidney failure and severe depression which signifies the removal of methyl red dye before discharging into the environment. Numerous adsorbents were investigated for the removal of Methyl red by various researchers were given in the Table 1.

Table 1: Degradation of Methyl red using Nano particles and agricultural waste.

Pollutant	Adsorbent used
Methyl red dye	Silica nano particles from rice husk
	Nano Fe_3O_4
	Ag-N-Co doppedZnOnanoparticles
	Tungsten trioxide thin films
	Boron and Nitrogen doped TiO_2
	Seaweed mediated zinc oxide Nanoparticles
	Spent oil shale

Activated carbon is widely used adsorbent for the removal of dyes and heavy metals, because it has large surface area, high micro porous structure, high adsorption capacity and special surface reactivity (Zhi et al. 2015). Various types of adsorbents are used to increase the degradation capacity in economic way. Many researchers made attempt on the development of adsorbents from various resources such as food waste, agricultural wastes, industrial wastes etc (Anjali et al. 2022). Natural materials from agricultural and industrial processes are abundant and could be used as low-cost adsorbents (Noho et al. 2020 Karunakaran and Thamilarasu, 2010). Because of their low cost, these materials can be disposed of without requiring costly regeneration after they have been used. Most of the low cost adsorbents have the limitation of low adsorption capacity and it generates more solid waste, which poses disposal problems.

The present work investigates the potential of *Ricinus Communis* stem activated by Silica gel for the degradation of synthetic textile dye Methyl red from wastewater. *Ricinus Communis* is species of flowering plant in spurge family, Euphorbiaceae and belongs to a monotypic genus, Ricinus and sub tribe, Ricninae (Manickavasagam, et al. 2013). *Ricinus Communis* grows throughout the drier parts and near drainages of India. Annual production of *Ricinus Communis* is estimated to be more than 1.0 tons globally, of which India accounts for 60% of the production (Makeswari and Santhi, 2013). The removal of heavy metals and dyes using various parts of *Ricinus Communis* were listed in the Table 2.

Table 2: Removal of heavy metals and dyes using various parts of *Ricinus communis.*

Pollutant	Precursors	Activating agent
	Castor bean seed	$ZnCl_2$
	Ricinus communis pericarp	H_2SO_4
	Ricinus communisepicarp	$ZnCl_2$
	Ricinus communis	Citric acid

Dyes	*Ricinus communis* pericarp	H_2SO_4
	Ricinus communis castor leafpowder (CLP)	Dried in a hot air oven for 5 h at 105ºC
Heavy metals	*Ricinus communis* pericarp	H_2SO_4
	Ricinus communis pericarp	H_2SO_4
	Ricinus communis leaves	Tannin gel
	Castor leaf *Ricinus communis* L powder	Dried and made to 63-µm particles
	Ricinus communis seed shell	Polypyrrole

2. MATERIALS AND METHODS

2.1.Adsorbent Material

The stem of Ricinus communis (RCS) was collected near Saravanampatti, Coimbatore District (Tamil Nadu). The adsorbent was thoroughly washed in running tap water to remove dirt and other particulate matter. The washed adsorbent was dried, powdered and stored in a airtight container for further studies.

2.2.Preparation of Adsorbent:

2.2.1.Preparation of Silica activated Ricinus Communis Stem (Si-RCS)

Ricinus communis stem powder is dissolved in water and agitated in a magnetic stirrer for 2 h. Silica is added to the slurry and agitation is continued for another 1h to attain homogeneity. The whole content is kept in a stable place for 8 h to obtain bubble free mixture. Ethanol and NaOH is added to the mixture and kept aside for 24 h to form the final product. The final product is filtered and dried in a hot air oven at 100˚C for 5 h. The dried product is packed in an airtight container for further studies (Narayanappa Madhusudhan et al. 2012).

2.2.2.Preparation of the adsorbate

A stock solution of Methyl red (1000ppm) was prepared separately and diluted to the various required initial concentrations.

2.3.Instrumentation

The instruments were used for the analysis of adsorbent and photocatalytic behavior are Digital pH meter, Conductivity bridge cell, Mechanical Bench Shaker, UV, SEM, EDX, XRD, FTIR and HPLC.

2.4.Characterization of the adsorbents

2.4.1.Physiochemical characterization of the adsorbents

Yield: The yield of the adsorbent in percentage was calculated by using the formula given below

$$Yield(Y) = (M/M_0) \times 100 \text{---------- (1)}$$

Where, M =Mass of the activated adsorbent, M_0=Mass of the adsorbent

2.4.2.Moisture content: About 5 g of the adsorbent was placed in a china dish, weighed, and heated for six hours at 110±20C. After heating, the dish was cooled in desiccators and weighed. Heating and cooling were performed every 30 minutes until there was less than a 5 mg difference between the two subsequent weights.

The moisture content is determined by loss in weight.

$$Moistue\ content\ (\%) = [(M - X)/M] \times 100 \text{---------- (2)}$$

Where M = Mass of the material taken for the analysis(g)

X = Mass of the materials taken after drying(g)

2.4.3.Adsorbent pH: About 0.2g of the adsorbent was weighed and taken in 50 ml beaker.30 ml of boiled and cooled water, whose pH was adjusted to 7.0,was added and heated to boiling.First10 ml of the filtrate, was rejected. The remaining filtrate was cooled and the pH was determined using digital pH meter.

2.4.4.Determination of Zero point charge (pHzpc): About 0.2g of adsorbent was added to a solution of Sodium nitrate of concentration 0.01M, whose pH is adjusted with 0.1M NaOH and 0.1M NaOH and 0.1M HNO_3 and final pH was measured. The results were plotted with initial pH vs. ΔpH (ΔpH =final pH-initial pH).The pH equals to zero yields pHzpc of the adsorbent.

2.4.5.Iodine Number

Determination of Iodine value of the adsorbents: Iodine solution was titrated against sodium thiosulphate (A) and with sample solution (B).

$$\text{Iodine value} = \text{C} \times \text{Conversion factor} \text{---------- (3)}$$

Where C = (B-A)

2.4.6.Surface acidity and Basicity of the adsorbent

Acidity: To 0.2g of adsorbent, 25 ml of 0.5M NaOH solution is taken in conical flask agitated it for 10 h in a closed flask. Filter it and the filtrate is titrated against with0.05M HCl. Acidity and Basicity is expressed in ‘m’moles/g.

Basicity: To 0.2 g of adsorbent,25ml of 0.5M HCl solution is taken in a conical flask ,agitated it for 10 h in a in a closed flask. Filter it and the filtrate is titrated against with 0.05M NaOH. Acidity and basicity is expressed in ‘m’ moles

2.4.7.Determination of surface group (Boehm titration)

Procedure

The adsorbent was well mixed with 20 ml of different base in volumetric standards. The adsorbent was added into 50ml conical flask and 20 ml of different bases added. The Flask is then sealed and agitated in shaker for 3 days. Filter this solution separately and 5ml of each filtrate is titrated with 0.1M HCl using water ethanol solution of methyl red as the indicator.

The number of basic sites calculated from amount of HCl reacted with the adsorbent material. Then the various free acidic groups present were derived using the assumption that NaOH neutralize carboxyl lactones and Na_2CO_3 neutralizes carboxyl and lactones and $NaHCO_3$ neutralizes only carboxyl groups respectively. The results obtained can be expressed in milli equivalents per gram (Jeyagowri Balakrishnan and Yamuna RangaiyaThiagarajan, 2021).

2.5. Photocatalytic studies

Batch mode adsorption studies for individual samples were carried out to determine the effect of different parameters such as pH, adsorbent dosage, dye concentration, contact time were studied. Batch adsorption studies were carried out using 250 mL flasks. The adsorbent and adsorbate solution were separated by using whatman 48 filter paper. The concentration of dye solution was measured by using UV-VIS spectrophotometer 119. All the experiments were duplicated and only the mean vales were reported. The maximum deviation observed was less than ±5% (Atef S. Alzaydien, 2009).

A stock solution of Methyl red (1000 ppm) were prepared and diluted to the various required initial dye concentrations. Degradation studies were carried out in the direct Sunlight during the month of March 2017 to May 2018. Batch mode studies carried out using required amount adsorbent dosage for each bottle and to this 50mL of solution of required concentration and pH of the solutions and kept in a shaker for 10 minutes to get homogeneous mixture, after getting the homogeneous mixture then they exposed to direct Sunlight. With regular time interval the resulting mixture was filtered using whatman 48 filter paper and the final concentration of Methyl red dye in the filtrate was estimated by UV-VIS spectrophotometer 119 at maximum absorbance of 524 nm respectively.

From the initial and final concentration, percentage of degradation was calculated by using the following equation

$$\% \text{ of Degradation efficiency} = \frac{A_0 - A_t}{A_0} \text{ ---------- (4)}$$

Where η was degradation ratio, $A_0$was the initial absorbance of the dye and A_t was the absorbance of the dye after degradation

2.5.1.Effect of pH

To analyze the effect of pH on the degradation of dye solutions, 50mL of 20 ppm concentration of dye solution were adjusted from 2 to 9 pH using 0.1M HCL and 0.1M NaOH, the optimum dosage of adsorbent was added and kept in the direct sunlight irradiation up to the equilibrium time. After exposed into the sunlight, the solution was filtered and the absorbance were measured by using UV-VIS spectrophotometer 119.

2.5.2.Effect of contact time

For the determination of rate of dye degradation by the studied adsorbent from 50 mL of 20 ppm of dye solution, the filtrate was analyzed for residual dye concentration at different time interval. The pH, adsorbent dosage and adsorbate concentration was kept constant[29].

2.5.3.Effect of Adsorbate concentration

The effect of adsorbate concentration was studied by varying the concentration of 50mL of the dye solution ranging from 20,40,60,80,100,120 and140 ppm. The equilibrium time and pH were kept constant depending on the dye solution under consideration.

2.5.4.Effect adsorbent dosage

The effect of adsorbent dosage ie., the amount of the adsorbents on degradation of dye was studied at various dosage ranging from 0.5 to0.35 g/ mL with 20ppm.The equilibrium time and pH were kept constant depending on the dye solution under consideration.

2.5.5.UV- Spectral studies

The degradation ability of Si-RCS was analyzed for the degradation of MR dye was confirmed by measuring the absorbance at regular time interval using UV-Visible spectrophotometer at wavelength of 524nm.

3. RESULTS AND DISCUSSION

3.1Characterization of the adsorbents

3.1.1.Physiochemical characterization of the adsorbent

The physiochemical properties of Si-RCS were evaluated and shown in Table 3.

Table 3 Physio-chemical characteristics of the Si -RCS

` Parameters	Values
Yield %	79.51
Moisture content %	6.22
pH	5.50
Surface acidity (mmoles/gm)	4.63
Surface basicity (mmoles/gm)	3.01
pH_{zpc}	4.00
Boehm titration (m.eq/gm) Basic sites	2.47
Phenolic and Carboxylic groups	1.32
Carboxyl groups	0.89

Iodine Number mg/g	2156.11

The total phenolic and carboxyl groups present in Si-RCS was 1.32 m.eq/gm. The yield and iodine number provide a measure of surface area or the capacity to get small molecules and are associated with the capacity to adsorb substances with low molecular weight and the pollutant uptake was high when the yield and iodine number were high. The high adsorbent moisture content demands a higher adsorbent load and also reduces the effectiveness of Si-RCS.

The negative charge density on the surface of Si-RCS is raised because the zero point charge for the investigated adsorbent is lower than the pH of the solution. Surface acidity and surface basicity values confirmed the presence of negative charge density. The presence of basic and oxygenated acidic surface groups on the adsorbent is explained by Boehm titration.

3.2.Surface characteristics

3.2.1.Scanning electron microscopic spectroscopy

The adsorbents surface features and properties were examined using scanning electron microscopy. SEM studies also reveal the surface texture and porosity of the adsorbent materials. SEM images of Si-RCS are shown in Fig 1. SEM images of the Si-RCS shows the porous and rough surface of the adsorbent. The rough surface and presence of pores in the surface of the adsorbent facilitates the adsorption of dye molecules on to the adsorbent surface.

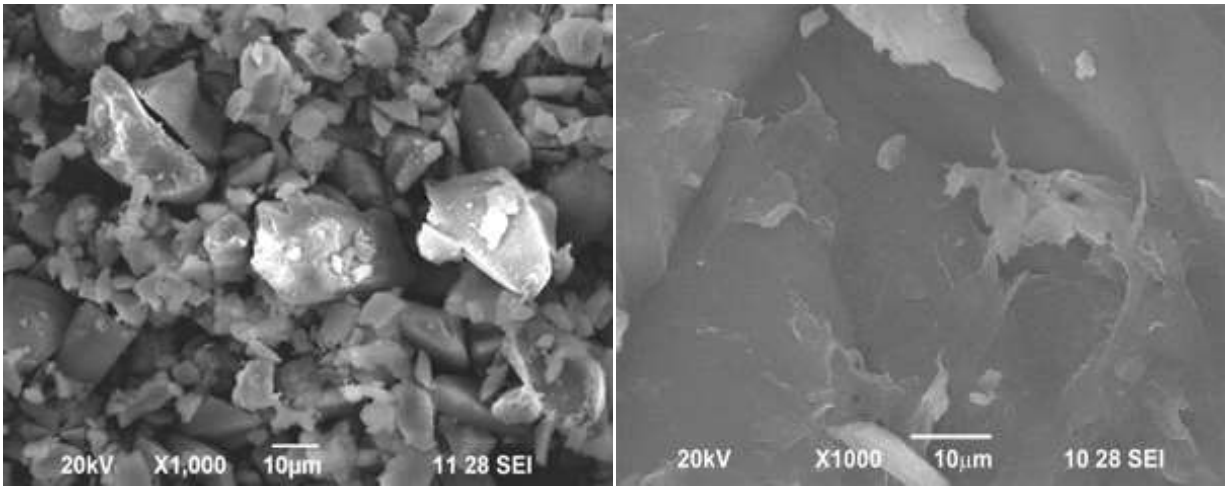

Fig. 1: SEM images of a) Si-RCS and b) Si- RCS after degradation of MR

3.2.2.Energy-dispersive –X ray Spectroscopy (EDS (or) EDX)

The fundamental principle is that each element has a unique atomic structure that permits a unique collection of peaks on its X-ray spectrum accounts for a major portion of the characteristics of energy-dispersive X-ray spectroscopy.

The conformation for the existence of elements for studied adsorbent (Si-RCS) were done by EDX analysis. The elements, percentage mass of elements presented in Si-RCS (before and after degradation), were represented in the Fig. 2, the values also were summarized in the Table 4.

Table 4 Composition of Si-RCS before and after degradation of MR

Compound	Si-RCS (Mass %)	Si-RCS-MR (Mass %)
C	25.03	32.75
O	24.62	28.02
Na	3.85	4.77
Si	42.38	10.91
Cl	-	23.47
Ca	4.12	-
S	-	0.08

Energy dispersive X-ray spectra showed the appearance of O, Na, C, Ca, K and Si in the adsorbent. These have been known as the principle elements of the adsorbent Si-RCS. The main elements were carbon and oxygen, whereas the carbon content is higher for Si-RCS than oxygen. The existence of Si in Si-RCS was due to the activation of RC stem with Silica gel.

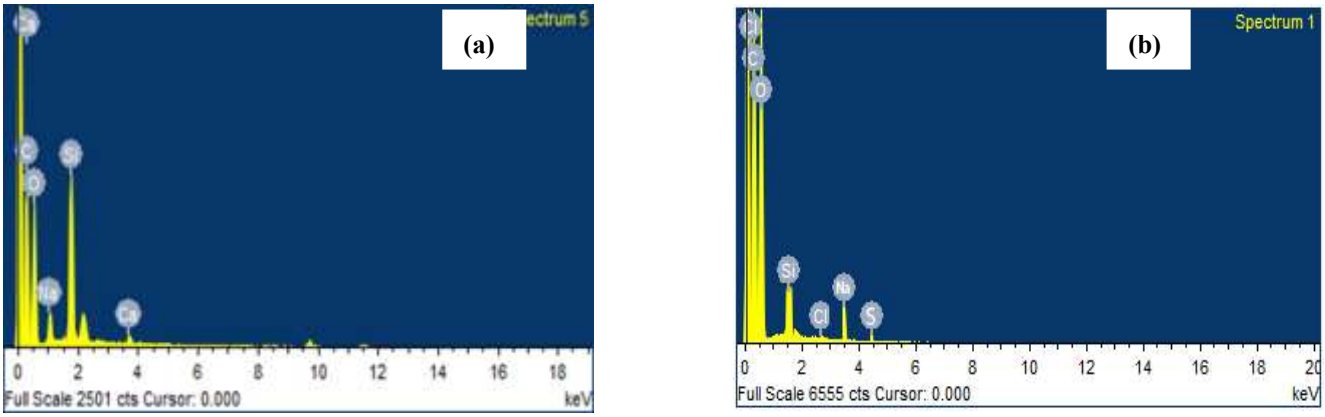

Fig. 2: EDX spectra of (a) Si-RCS and (b) Si-RCS after degradation of MR

3.2.3.X-Ray Refractory Diffraction (XRD)

The structure of the adsorbent RCS is complex and includes both crystalline and amorphous regions. RCS displays an XRD pattern (Fig. 3a) that is comparable to that of other cellulosic materials. The smallest peak (at around 16^0) denotes a less ordered polysaccharide structure, while the biggest peak (at about 22^0) shows the existence of highly organized cellulose.

Fig. 3b shows the XRD pattern of Silica activated RCS. Following silica activation, the crystalline character of RCS was enhanced, as evidenced by the rise in peak intensity in the Si-RCS XRD pattern. However there are no significant changes in XRD pattern of the Si- RCS after MR degradation.

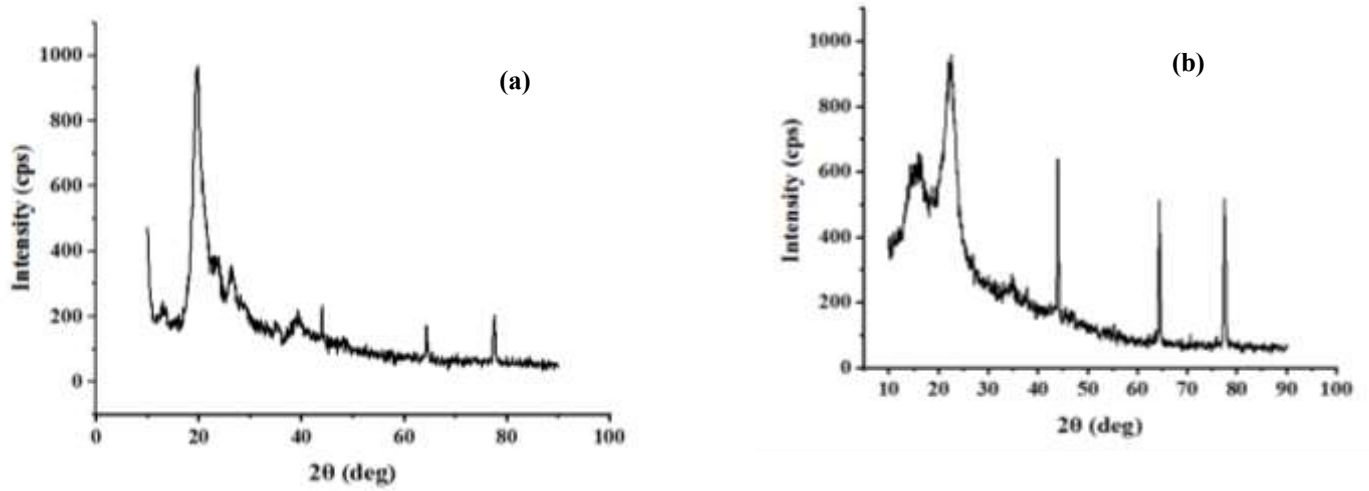

Fig. 3: XRD image of a) RCS and b) Si-RCS

3.2.4.Fourier Transform and Infrared Spectroscopy (FTIR)

The purpose of employing FTIR analysis was used to determine the presence of functional groups with the help of characteristic peaks. Fig. 4a and 4b shows the FTIR spectra of RCS and Si-RCS respectively. The FTIR of Si-RCS spectra exhibit changes in peak intensity and modest peak-position shifting confirming the silica activation.The FTIR spectra of Si-RCS contain a band between 3171 cm^{-1}shows the existence of NH groups. A peak at 2878 cm^{-1} indicates the presence symmetric and asymmetric vibration of methyl and methylene group. The peak around 2338.82 to 2353.59 cm^{-1}indicates the presence of C≡C stretching due to silica activation. The region of 1505 cm^{-1} assigned to stretching vibrations of aromatic structure C=C in lignin and the peak at 1054.06 cm^{-1} indicates the presence of lignin.

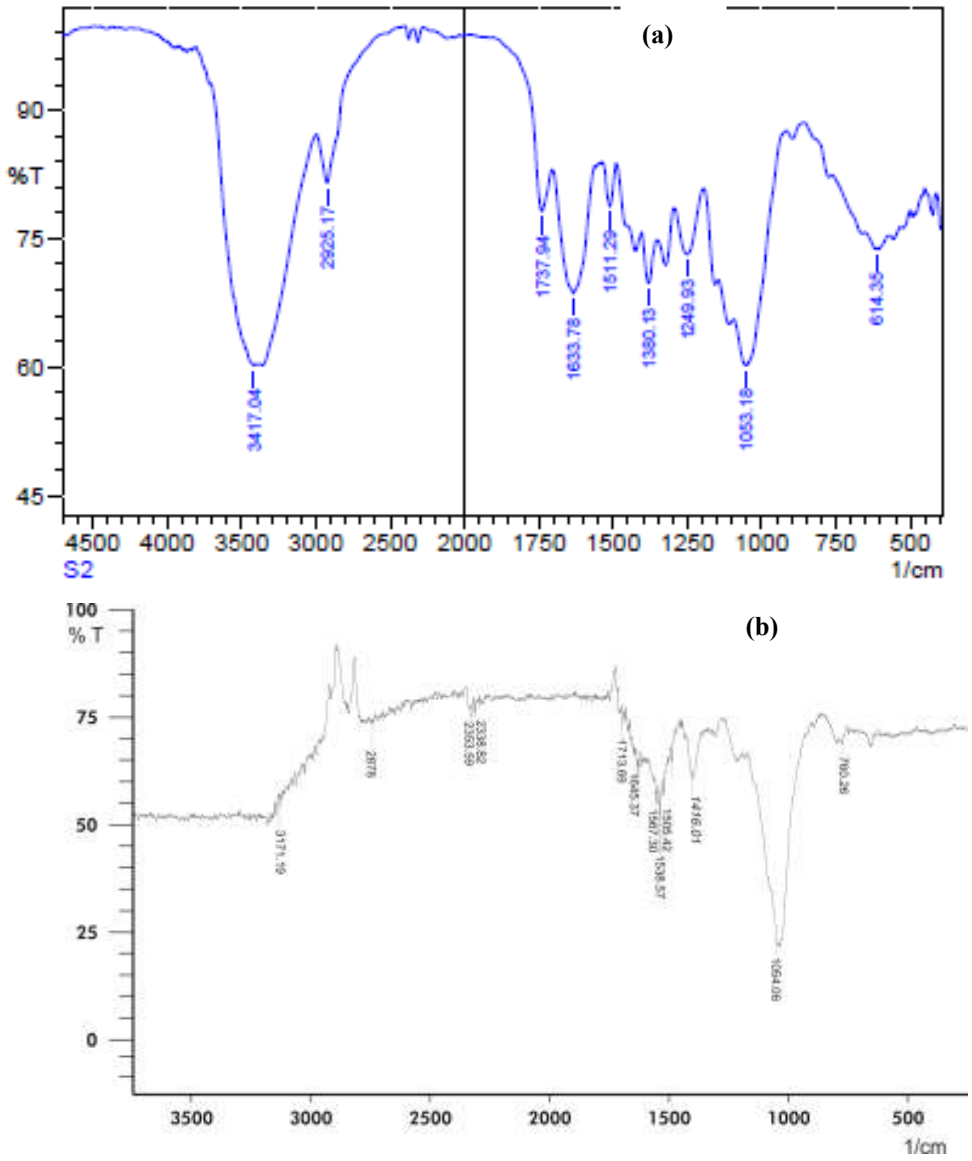

Fig. 4: FTIR image of a) RCS and b) Si-RCS

3.3. PHOTO CATALYTIC STUDIES

3.3.1.Effect of Initial dye concentration

The effect of initial dye concentration of MR onto Si-RCS was studied using initial dye concentration ranges from 20ppm-140ppm. The experimental studies indicate the decrease in dye degradation with increase in dye concentration and are represented in the Fig. 5. The degradation efficiencies were found to decline with increase in initial concentration of MR dye solution on Si-RCS. The degradation efficiency of MR onto Si-RCS was decreased from 85.85% to 28.98%. The decline in degradation was due to the lack of active sites on the adsorbent surface at

higher initial concentration of MG and MR, the ratio of initial number of moles of dye molecules to the available adsorption surface area was high. This may be responsible to an increase in the driving force of concentration gradient with the rise in initial dye concentration.

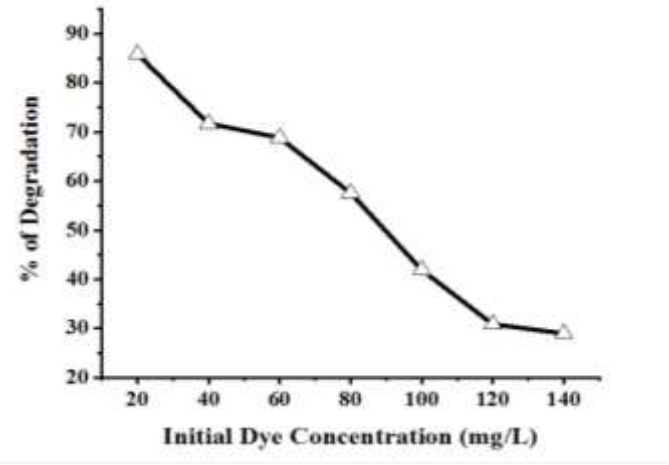

Fig. 5: Effect of Initial Dye concentration on adsorption of MR on Si-RCS

3.3.2. Effect of solution pH:

The adsorption process was influenced by pH of the aqueous dye solution. pH was the important factor which decides the ionising capability of the adsorbing molecules at the current pH. The effect of initial pH of MR dye solution on the amount of adsorption was studied by varying the initial pH for the adsorbent Si-RCS under optimum conditions. The optimum dose of adsorbent was fixed as 0.2g, 0.25g and 0.2g and the optimum initial dye concentration was 20ppm of Si-RCS respectively. The optimum contact time of Si-RCS was 100 minutes for the degradation of MR.

The maximum adsorption capacity of the adsorbents with respect to the initial pH of the adsorbate was depicted in the Fig. 6. The adsorption capacity decreased with increasing in solution pH and the optimum pH value for the adsorption of MR on Si-RCS was 4.The maximum degradation efficiencies of MR on Si-RCS was 80.58% at pH 6 and 85.85% at pH 3 respectively.

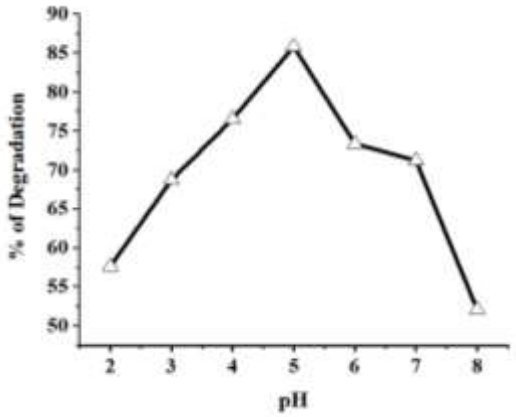

Fig. 6: Effect of pH on adsorption of MR on Si-RCS

3.3.3.Effect of contact time

The percentage degradation was found to increase with increasing contact time and then it becomes stable after attainment of equilibrium time as so the maximum degradation achieved at 100 minutes for Si-RCS. This may be due to the fact that initially surface of adsorbent sites were highly vacant and solute concentration was high, and after the equilibrium time there was no change in the degradation of MR onto the studied adsorbents, because the active sites are lesser in the surface of the adsorbent at this stage. The maximum degradation efficiency of MR onto Si-RCS was 85.85% at 100 mins. The effect of contact time for the degradation of MR onto Si-RCS is revealed in the Fig. 7.

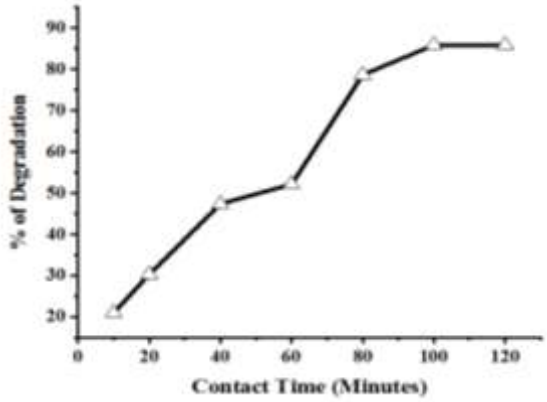

Fig.7: Effect of Contact time on adsorption of MR on Si-RCS

3.4. Isotherm Modelling

Adsorption isotherm generally explains the dynamic behaviour of any adsorbate from solution to the solid adsorbent phase. The efficiency of adsorbent for a particular adsorbate removal is represented by adsorption isotherms.

The equilibrium data analysis is important to develop the equation which exactly indicates the results that can be used for the designing purposes (Jeyagowri Balakrishnan and Yamuna Rangaiya Thiagarajan, 2015).The adsorption capacities of

the adsorbent are determined by equilibrium studies. To correlate the quantity of adsorption and liquid phase concentration Langmuir, Freundlich, Temkin and Dubinin-Radushkevich (D-R) adsorption isotherm equations were used. The adsorption isotherm models are predicted from the values of correlation regression coefficient (R^2).

3.4.1.Langmuir Isotherm

Irving Langmuir developed the Langmuir isotherm in 1916 to explain the nature of the surface coverage of an adsorbed gas on the pressure of the gas on the surface at constant temperature. The monolayer adsorption on the homogeneous surface of the adsorbent by dye molecules is the main assumption of Langmuir model (Jeyagowri and Yamuna, 2016).

The mathematical expression the Langmuir adsorption isotherm is

$$\frac{C_e}{q_e} = \frac{1}{q_{max}} b + \frac{C_e}{q_{max}} \quad \text{---------- (5)}$$

Hence C_e is the concentration of MR dye solution (mg/L), q_e is the concentration of MR in adsorbent (mg/g), q_{max} is the maximum adsorption capacity (mg/g) and b is the Langmuir equilibrium constant. The linear plot of C_e/q_e vs C_e gives a straight line with a slope of $1/q_{max}$ and the intercept C_e/q_{max} were shown in the Fig. 8.

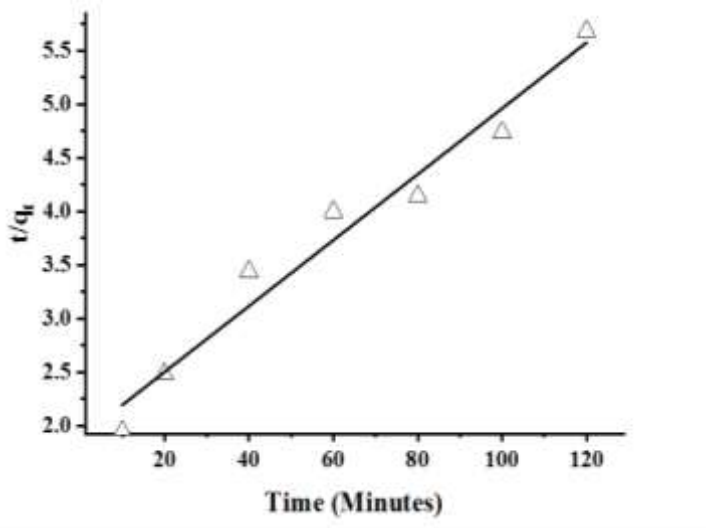

Fig. 8: Langmuir isotherm for adsorption of MR on Si-RCS

The isotherm parameters obtained from the Langmuir model the removal of MR onto Si-RCS were shown in the Table 3. The calculated and the experimental values of this model are very close to each other, which show the parameters were well fitted for Langmuir adsorption isotherm model. The correlation regression coefficient is the best evidence for the adsorption of MR onto Si-RCS follows the Langmuir isotherm. The R^2values for the adsorption of MR onto Si-RCS were 0.991.

3.4.2.Freundlich isotherm

The Freundlich adsorption isotherm model is the well-known equation to explain the adsorption process. The multilayer adsorption and heterogeneous surface of the adsorbent for non-ideal adsorption can be described by a Freundlich empirical equation. The linear form of Freundlich isotherm is given as follows

$$\text{Log } q_e = 1/n \log(C_e) + \log K_f \text{---------} (6)$$

Where K is the Freundlich constant (mg/g), n is the Freundlich exponent, q_e is the amount of adsorbed per unit mass of the adsorbent and C_e adsorbate concentration at equilibrium in solution (mg/lit). The Freundlich constant K_f and 1/n was calculated from the slope and intercept from the plot of $\log C_e$ vs $\log q_e$ for the adsorption of MR onto Si-RCS. K_f was approximately an indicator of the adsorption capacity related to the bond energy and 1/n was the intensity of dye adsorption onto the adsorbent surface (Rajeswari Arunachalam *etal*. 2012). The extent of the exponent, 1/n value suggested the favourability of the adsorption. The value of 1/n <1 represent favourable adsorption condition, while 1/n >1 represent the cooperative adsorption. The calculated data obtained from Freundlich adsorption isotherm of the MR onto Si-RCS were summarized in the Table 5. The Langmuir and Freundlich isotherm models were correlated by the regression coefficients (R^2). The correlation coefficient values of MR onto Si-RCS for Langmuir and Freundlich isotherm is 0.991 and 0.924. From the results Langmuir adsorption isotherm was well fitted when compared to Freundlich isotherm model and confirms the monolayer adsorption of the dye onto the adsorbent (Pradeeba and Sampath, 2017).

Table 5 Isotherm parameters for adsorption of MR onto Si-RCS

Dye		Methyl Red
Langmuir Isotherm	Q_m (mg/g)	9.58
	b (L/mg^{-1})	3.86
	R^2	**0.991**
Freundlich Isotherm	K_F(L/g)	2.912
	n	3.13
	R^2	**0.924**
Temkin Isotherm	α	0.637
	β	1.94
	R^2	**0.905**
D-R Isotherm	E (kJ/mol)	1.000
	R^2	**0.9195**

3.4.3.Temkin adsorption isotherm

Temkin isotherm describes the effect of some indirect adsorbent/adsorbate interactions on adsorption isotherm indicates that the heat of adsorption decreases linearly with coverage. The simplified form of Temkin isotherm is as follows

$$q_e = \beta \ln\alpha + \beta \ln C_e \text{---------- (7)}$$

Where β = (RT)/b, where b is the constant related to heat of adsorption (L/mg), α is the binding equilibrium constant, T is the absolute temperature (K), R is the universal gas constant (8.314 J), q_e is the amount of adsorbed per unit mass of the adsorbent and C_e is the concentration of the adsorbate in solution at equilibrium condition. The values of α, β and R^2 obtained from the plot of lnCe vs q_e of adsorption of MR onto Si-RCS were presented in Table 5.

3.4.4.Dubinin- Radushkevich Isotherm (D-R isotherm)

The adsorption capacity of the adsorbent is determined by using Dubinin- Radushkevich Isotherm model. The mathematical expression of D-R model is given as follows.

$$\boldsymbol{ln q_e = ln q_{max} - \beta \varepsilon^2} \text{---------- (8)}$$

Where q_{max} is the theoretical saturation capacity and ε is the Polanyi potential. The constants β and q_{max} can be calculated from the graph plotted between ε^2 vs lnq_e for the adsorption of MR onto Si-RCS and are presented in Table 5. The constant β provides the mean free energy 'E' of adsorption per molecule of dye, when it is shifted to the solid surface of the adsorbent from infinity in the solution. The value of E would provide information about the nature of adsorption – whether it is physisorption or chemisorption. The adsorption process is physisorption when E lies between 1and 8 KJ mol^{-1}, while it is chemisorption when E is higher than 8 KJ mol^{-1}. From Table 3, it was observed that the value of E is 1.000 KJ mol^{-1} confirming that a weak physical force of interaction is the driving force of the adsorption of dye onto Si-RCS (Pradeeba and Sampath, 2022).

From Table 3, it is revealed that the correlation coefficient R^2 of Freundlich, Temkin, D-R isotherm were lower than Langmuir adsorption isotherm for dye indicating that the monolayer adsorption of the dye onto the surface of the adsorbent.

3.5.Kinetic Modelling

3.5.1.Pseudo second order kinetics

The adsorption kinetics of MR onto Si-RCS was explained by using pseudo second order kinetics. The pseudo second order equation is

$$\frac{t}{q_t} = \frac{1}{K_2} - \frac{t}{q_e} \text{---------- (9)}$$

where K_2 is the equilibrium rate constant for the pseudo second order adsorption (g/mg min) can be calculated from the slope of the graph was shown in the Fig.9 and the experimental data were summarized in the Table 6.The initial adsorption rate and the rate constant k for the pseudo second order can be calculated from $h=kq_e^2$(mg/g min) (Vidhya et al.. 2023). From the intercept and slope, the value of $q_{e,}$ k and h can be calculated. The experimental data and the plot were well fitted for the pseudo second order kinetic model. The correlation regression coefficient R^2 and maximum adsorption capacity $q_e$of the adsorption of MR was 0.9655 and 19.68. The calculated $q_e$values are well agreed with the experimental data. From the experimental result it is evident that the adsorption system followed the pseudo second order kinetic model and it provided good correlation for the adsorption of MR onto Si-RCS (Indra DeoMall *etal.* 2005).

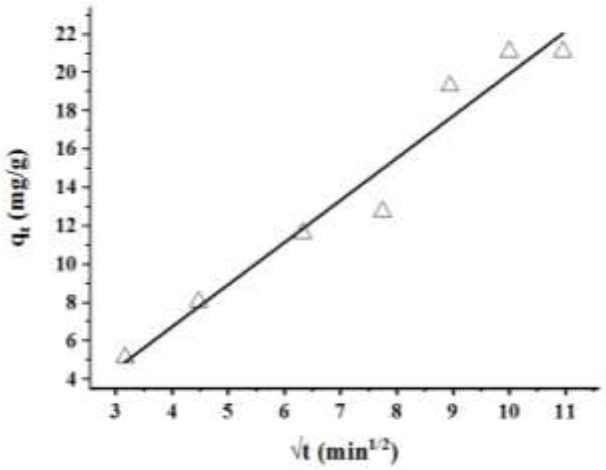

Fig.9: Pseudo second order model for adsorption of MR on Si-RCS

3.5.2.Elovich equation

The Elovich equation is another rate equation that is typically used to illustrate the adsorption capacity. The equation is exhibited as

$$\frac{dq_t}{\mathrm{dt}} = B_E \exp\left(-A_E q_t\right) \text{ ---------- (10)}$$

Where A_E is the elution constant (g/mg) and B_E is the initial adsorption rate [mg(g/min)]. A graph is plotted between lnt vs q_t and the experimental data were summarized in the Table 6. The elution constant A_E and initial adsorption rate B_E for the adsorption of MR was 0.126 and 2.41 for Si-RCS respectively. The elution constant A_E is lower than the initial adsorption rate which contributes to the more adsorption capacity of MR onto Si-RCS.

3.5.3.Intra particle diffusion model

The intra particle diffusion model is the important tool to find out the mechanism of adsorption process. The intra particle diffusion model is expressed as

$$q_t = K_d t^{1/2} + C \text{ ---------- (11)}$$

Where C is the intercept, K_d intra particle diffusion rate constant (mg/g $min^{1/2}$) and q_t is the amount of MR dye adsorbed at time, t(mg/g). A plot of qt vs √t gives a linearized form of intra particle diffusion model for adsorption of MR by Si-RCS were studied and the values were summarized in Table 4. From the results the intra particle diffusion rate enduring K_d, intercept C and regression correlation coefficient R^2 of MR onto Si-RCS was 2.22 to 2.05 and 0.9593 respectively. The value C (intercept) gives information about the thickness of the boundary layer, if the resistance of the external mass transfer increases the thickness of the boundary layer also increases (Pradeeba and Sampath, 2022). In case of intra particle diffusion model, it is necessary for the qt vs √t plots to pass through the origin if the intraparticle diffusion is the rate limiting step. The plot of qt vs √t for the adsorption of MR by Si-RCS does not pass through the origin which indicates that the intraparticle diffusion model is not rate limiting step as surface adsorption and intraparticle diffusion were concurrently operating during the dye and adsorbent interaction. The comparison of correlation regress coefficient values for Si-RCS for the adsorption of MR were summarized in the Table 6.

The pseudo second order kinetic model gives the good correlation for all of the adsorption process of MR onto Si-RCS.

Table 6 Kinetic parameters for the adsorption of MR onto Si-RCS

Dye	Kinetic models	Parameters	Si-RCS
Methyl Red	Pseudo- first order equation	$k_1(min^{-1})$	0.076
		q_e(mg/g)	14.12
		R^2	**0.8233**
	Pseudo-Second order equation	$k_2(Lmole^{-1}\ sec^{-1})$	0.0013
		h	0.503
		q_e,cal(mg/g)	19.68
		R^2	**0.9655**
	Elovich Model	A_E (mg/g)	0.126
		B_E (mg/g)	2.41
		R^2	**0.911**
	Intra particle diffusion	k_d (mg/g)	2.22
		R^2	**0.9593**
		C	-2.05

3.6.Mechanism of dye degradation

The prime reason for using activated *Ricinus Communis* Stem as a photo catalyst for the degradation of MR dyes is when it is exposed to direct solar light irradiation it gives electron hole pairs. The dye degradation process is induced by the formed electron hole pairs. Even though it is photocatalytic degradation, initially adsorption of the dye on the surface of the adsorbent occurs followed by photo degradation process. In the early stages, when the dye concentration is low, there are more vacant sites available on the adsorbent's surface for adsorbing dye molecules; however, as the dye concentration increases, there are fewer vacant sites available on the adsorbent's surface for adsorbing dye molecules. Because, the vacant sites are filled by the dye molecules therefore the rate of dye degradation decreases (Pradeeba *etal.* 2022). Mechanism of photo degradation occurs in two steps, i.e., Dye adsorption by adsorbent followed by degradation under direct sunlight takes place by the following equation

- Adsorbent+ hν → Adsorbent (e^-+h^+) ---------- (12)
- O_2+ e^- →$O_2^{\cdot-}$---------- (13)
- $O_2^{\cdot-}$ + e^- + $2H^+$ → 2OH ˙----------(14)

Oxygen plays a vital role in the degradation of dyes. The sunlight, oxygen and hydroxyl ion shows considerable effects on the degradation. The degradation capacity of the dye is reduced if any of the above parameters is reduced. The formed hydroxyl radical species react with any species to form hydrogen peroxide, which is a considerable active species in photo degradation process. Fig.10 shows the photocatalytic degradation of the dye MR by the adsorbent SiRCS

- 2OH ˙ →H_2O_2 ---------- (15)

The formed hydrogen peroxide cleaved to form OH ˙

- H_2O_2 + hν → 2OH ˙---------- (16)

Degradation of dye by OH ˙ radical

- OH ˙$_{ads}$ + dye → oxidation of the dye ---------- (17)

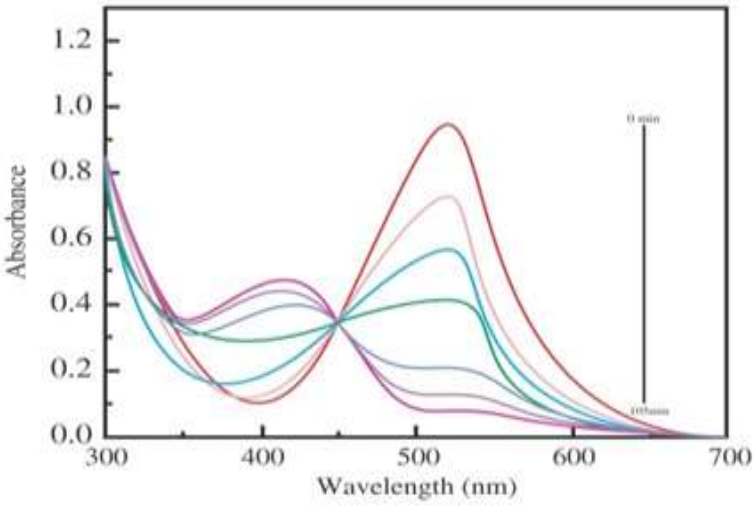

Fig. 10: Photocatalytic degradation of MR on Si-RCS

4. CONCLUSIONS

In the present research work, Silica gel activated adsorbent prepared from *Ricinus communis* stem (Si-RCS). The photocatalytic removal of methyl red dye using (Si-RCS) in the presence of natural sunlight was examined. The effectiveness of methyl red dye degradation depends on initial dye concentration, contact time, and pH. In the dye concentration variation, the maximum degradation efficiency was 86% in the presence of natural sunlight and the optimum dye concentration was 20 ppm at 0.25 g photocatalyst dosage. The adsorbent Si-RCS were utilized as a catalyst in the existence of natural sunlight to investigate kinetic isotherm, pseudo-first-order and pseudo-second-order for dye variation. The best fit model was found to be pseudo second order based on the R^2 value. Adsorption isotherms like Langmuir and Freundlich. Temkin and DR isotherm has been analyzed for dye variation parameter in the removal of Methyl Red. Among the isotherm models studied, it was found that Langmuir is the best fit model.

Author Contributions:

Conceptualization: Dr. V. Nirmala Devi.; Methodology, Dr. B. Jeyagowri.; SoftwareDr. S. J. Pradeeba; Validation, Dr. V. Nirmala Devi.;Formal analysis, Dr. S. J. Pradeeba; Investigation Dr. V. Nirmala Devi..; Resources, Dr. B. Jeyagowri.; Data curation, Dr. N. Nithiya.; Writing—original draft preparation, Dr. L. Vidhya; Writing—review and editing, Dr. L. Vidhya.; Visualization, Dr. S. J. Pradeeba.; Supervision, Dr. N. Nithiya.

All authors have read and agreed to the published version of the manuscript.

Conflicts of Interest: "The authors declare no conflicts of interest."

REFERENCES

1. Anjali, K.P., Raghunathan, R., Geetha Devi. and Susmita Dutta. 2022. Photocatalytic degradation of methyl red using seaweed mediated zinc oxide nanoparticles. *Biocatalyst and Agricultural biotechnology*, 43,pp.102384-102391.https://doi.org/10.1016/j.bcab.2022.102384

2. Ait oukharaz, N., Lakhmiri, R., El Fargani, H., Eladnani, I., Sguillar, M., Albourine, A., Bazzi, V., Safi, M., Cherkaoui, O. 2023, Application of Castor plant (Ricinus communis. L) as a green sorbent for removing cationic dyes from textile effluents, *Moroccan Journal of chemistry*, Vol. 11 (04) pp. 897-1318. https://doi.org/10.48317/IMIST.PRSM/morjchem-v11i04.43414
3. Atef S. Alzaydien. 2009.Adsorption of Methylene Blue from Aqueous Solution onto a Low-Cost Natural Jordanian Tripoli.*Americal Journal of Applied science*, 6(6), pp. 1047-1058.https://doi.org/10.3844/ajassp.2009.1047.1058.
4. Galenda, A., Crociani, L., El Habra N., Favaro, M., Natile, M.M. and Rossetto, G. 2014. Effect of reaction conditions on Methyl red dye degradation. *Applied surface science*, 314, pp. 919-926. https://doi.org/10.1016/j.apsusc.2014.06.175
5. Hameed, B. H. and El-khaiary, M. I. 2008. Malachite green adsorption by rattan sawdust: Isotherm, kinetic and mechanism modeling. *Journal of Hazardous Materials*, 159 (2-3), pp. 574-579.https://doi.org/10.1016/j.jhazmat.2008.02.054
6. Hasan, M., Ahmad, A.L. and Hameed, B.H. 2008.Adsorption of reactive dye onto cross-linked chitosan/oil palm ash composite beads.*Chemical Engineering Journal*, 136 (2-3), pp.164-172.https://doi.org/10.1016/j.cej.2007.03.038
7. Hunge, Y.M., Mohite, V.S., Kumbhar, S. S., Rajpure, K.Y., Moholkar, A.V. and Bhosale. C.H. 2015. Photoelectrocatalytic degradation of methyl red using sprayed WO_3 thin films under visible radiations, *Journal of Material science*, 26, pp. 8404-8412.http://dx.doi.org/10.1007/s10854-015-3508-z
8. Indra DeoMall., Vimal ChandraSrivastava., Nitin Kumar., Agarwal. and Indra ManiMishra. 2005. Adsorptive Removal of Malachite Green Dye from Aqueous Solution by Bagasse Fly Ash and Activated Carbon – Kinetic Study and Equilibrium Isotherm Analyses. *Colloids and Surfaces A Physicochemical and Engineering Aspects*, 264(1-3), pp. 17-28.https://doi.org/10.1016/j.colsurfa.2005.03.027
9. Jeyagowri Balakrishnan. and Yamuna RangaiyaThiagarajan. 2021. Characterization And Potential Suitability Of Simarouba Glauca Seed Shell Lignocellulosic Biomass As Adsorbent Of Basic Dyes From Aqueous Solutions. *Cellulose chemistry and Technology*, 55 (5-6), pp. 705-722. https://doi.org/10.35812/CelluloseChemTechnol.2021.55.60
10. Jeyagowri Balakrishnan. and Yamuna RangaiyaThiagarajan.2015. Biosorption of methylene blue from aqueous solutions by modified mesoporous Simarouba glauca seed shell powder, *Global Nest Journal*,17(4), pp. 701-715.https://doi.org/10.30955/gnj.001723.
11. Jeyagowri, B. and Yamuna R.T . 2016. Potential efficacy of a mesoporous biosorbent Simarouba glauca seed shell powder for the removal of malachite green from aqueous solutions. *Desalination and water treatment*,57(24), pp. 11326-11336.https://doi.org/10.1080/19443994.2015.1042060
12. Karthikeyan, S., Jambulingam, M., Sivakumar, P., Shekhar, A. P. and Krithika, J. 2006.Impacts of Textile Waste Water on Fingerlings of Fresh Water Reservoir, *Asian Journal of Chemistry*, 25(16), pp. 303-312.http://dx.doi.org/10.14233/ajchem.2013.15534
13. Karunakaran, K. and Thamilarasu, P. 2010. Removal Of Fe(III) From Aqueous Solutions Using Ricinus Communis Seed Shell And Polypyrrole Coated Ricinus Communis Seed Shell Activated Carbons. *International journal of Chemtech Research*, 2(1), pp.26-35. https://sphinxsai.com/sphinxsaiVol_2No.1/ChemTech_Vol_2No.1/ChemTech_Vol_2No.1PDF/CT=06(26-35)_JAN-MAR_2010.pdf
14. Madhavakrishnan, S., Manickavasagam, K., Vasanthakumar, R ., Rasappan, K., Mohanraj, R. and Pattabh S .2009. Adsorption of Crystal Violet Dye from Aqueous Solution Using Ricinus Communis Pericarp Carbon as an Adsorbent. *Journal of chemistry*, 6, pp. 1109-1112.https://doi.org/10.1155/2009/764197
15. Makeswari, M. and Santhi, T. 2013. Removal of Malachite Green Dye from Aqueous Solutions onto Microwave Assisted Zinc Chloride Chemical Activated Epicarp of Ricinus communis. *Journal of water resource and protection*, 5(2), pp. 222-234. http://dx.doi.org/10.4236/jwarp.2013.52023.

16. Manickavasagam, K., Dhanakumar, S., Chandrasekar, P., Narayanan, P.R. and Pattabhi.S. 2013. Removal of Reactive yellow from aqueous solution by using Ricinus Communis pericarp carbon as an adsorbent. *International Journal of advancement in Life Science Research*, 6, pp. 404-416.https://scholar.google.com/citations?view_op=view_citation&hl=lt&user=dik6028AAAAJ&citation_for_view=dik6028AAAAJ:u5HHmVD_uO8C
17. Monda, S. 2018. Methods of Dye Removal from Dye House Effluent—An Overview. *Environmental Engineering Science*., 25, pp. 383-396.**https://doi.org/10.1089/ees.2007.0049**
18. Narayanappa Madhusudhan., KambalagereYogendra. and Kittappa M. Mahadevan. 2012. Photocatalytic Degradation of Violet GL2B Azo dye by using Calcium Aluminate Nanoparticle in presence of Solar light. *Research Journal of chemical science*, 2(5), pp. 72-77.http://dx.doi.org/10.13140/RG.2.2.18039.06568
19. Noha Ahmed Mahmoud., EhssanNassef. and Mohamed Husai. 2020.Use of spent oil shale to remove methyl red dye from aqueous solutions. *AIMS material science*,27 (3), pp. 338-353.https://doi.org/10.3934/matersci.2020.3.338
20. Pradeeba, S.J. and Sampath, K. 2022. Depollution of Synthetic dyes From Wastewater Using Polyazomethine/TiO_2 And Polyazomethine/ZnO Nanocomposites Via Photocatalytic Process. *Global Nest Journal*, 24 (3), pp. 407-413.https://doi.org/10.30955/gnj.004268
21. Pradeeba, S.J. and Sampath, K. (2022). Photodegradation, thermodynamic and kinetic study of cationic and anionic dyes from effluents using polyazomethine/ZnO and polyazomethine/TiO_2 nanocomposites. *Journal of Optoelectronic and Biomedical Materials*,14(3), pp. 89-105.https://chalcogen.ro/89_PradeebaSJ.pdf.
22. Pradeeba, S.J. and Sampath, K. 2017. Synthesis and Characterization of Poly(azomethine)/ZnO Nanocomposite Toward Photocatalytic Degradation of Methylene Blue, Malachite Green, and Bismarck Brown. *Journal of Dynamic system, measurement and control*, 141(5), 051001-13.https://doi.org/10.1115/1.4042090
23. Pradeeba, S.J., Sampath, K. and Jeyagowri, B. 2022. Kinetic and adsorption isotherm modeling of photodegradation of anionic dyes using polyazomethine/titanium dioxide and polyazomethine/zinc oxide nanocomposite.*Desalination and water treatment*, pp.262-282.https://doi.org/10.5004/dwt.2022.28590.
24. Rajeswari Arunachalam.,Sujatha Dhanasingh. and Balasaraswathi Kalimuthu. 2012. Phytosynthesis of silver nanoparticles using Coccinia grandis leaf extract and its application in the photocatalytic degradation. *Colloids and Surfaces B: Biointerfaces*. 94(1), pp. 226-230.https://doi.org/10.1016/j.colsurfb.2012.01.040
25. Rimsha Jameel., Saima Lashari., Muhammad Nabeel Sharif., Shabnam Javaid., Kashif Alam., Faisal Mahmood., Waqar Ahmad., Aneeza Kokab. 2024. Effective Sequestration of Acid Orange-7 Dye from Wastewater by using Ricinus Communis Biochar along with Zinc Oxide Nanocomposites.*Indus Journal of bioscience research*, Vol. 2(02). https://doi.org/10.70749/ijbr.v2i02.363
26. Sandip Kumar Panda and Lalit Prasad. 2020. Fe_3O_4 Based Nanoparticles as a Catalyst in Degradation of Dyes: A Short Review. *International Journal of Advanced research in science, communication and Technology*„11(2), pp.34-41.http://dx.doi.org/10.48175/594
27. TesfayWelderfael, O.P., Yadav, Abi M., Taddesse. and Jyotsna Kaushal. 2013. Synthesis, characterization and photocatalytic activities of Ag-N-codoped ZnO nanoparticles for degradation of methyl red, *Bulletin of the chemical society of Ethiopia*, 27(2), pp. 221-232.http://dx.doi.org/10.4314/bcse.v27i2.7
28. Vinoda, B. M., Vinuth, M., Yadav. D. Bodke . and Manjanna, J. 2015.Photocatalytic Degradation of Toxic Methyl Red Dye Using Silica Nanoparticles Synthesized from Rice Husk Ash. *Journal of Environmental and Analytical toxicology*, 5 (6), pp. 1-4.http://dx.doi.org/10.4172/2161-0525.1000336
29. Vidhya,L. , Vinodha, S. Pradeeba S.J. Jeyagowri, B, Nirmaladevi, V. and Nithiya.N., 2023. Adsorption and Kinetic Studies on Sequestering Effect of Porous Biodegradable Biochar Obtained from Pig-Bone on Hexavalent Chromium from Aqueous Solution, *Nature Environment and pollution technology*, 22(2), pp.681-690.

30. Zhi Lee Lin. and Muhammad Abbas Ahmad Zaini. 2015. Metals Chloride-Activated Castor Bean Residue for Methylene Blue Removal, *J. Tekno*., 74 (7), pp. 65-74. https://doi.org/10.11113/jt.v74.4700.